Novel protease inhibitor-loaded Nanoparticle-in-Microparticle Delivery System leads to a dramatic improvement of the oral pharmacokinetics in dogs

 CrossMark

Julieta C. Imperiale [a], Pablo Nejamkin [b], Maria J. del Sole [b], Carlos E. Lanusse [b, c], Alejandro Sosnik [d, *]

[a] Department of Pharmaceutical Technology, Faculty of Pharmacy and Biochemistry, University of Buenos Aires, Buenos Aires, Argentina
[b] Small Animal Teaching Hospital, Faculty of Veterinary Sciences, National University of Central Buenos Aires, Tandil, Argentina
[c] National Science Research Council (CONICET), Buenos Aires, Argentina
[d] Group of Pharmaceutical Nanomaterials Science, Department of Materials Science and Engineering, Technion-Israel Institute of Technology, Technion City, Haifa, Israel

ARTICLE INFO

ABSTRACT

With the advent of the Highly Active Antiretroviral Therapy, the morbidity and the mortality associated to HIV have been considerably reduced. However, 35—40 million people bear the infection worldwide. One of the main causes of therapeutic failure is the frequent administration of several antiretrovirals that results in low patient compliance and treatment cessation. In this work, we have developed an innovative Nanoparticle-in-Microparticle Delivery System (NiMDS) comprised of pure drug nanocrystals of the potent protease inhibitor indinavir free base (used as poorly water-soluble model protease inhibitor) produced by nanoprecipitation that were encapsulated within mucoadhesive polymeric microparticles. Pure drug nanoparticles and microparticles were thoroughly characterized by diverse complementary techniques. NiMDSs displayed an encapsulation efficiency of approximately 100% and a drug loading capacity of up to 43% w/w. In addition, mucoadhesiveness assays *ex vivo* conducted with bovine gut showed that film-coated microparticles were retained for more than 6 h. Finally, pharmacokinetics studies in mongrel dogs showed a dramatic 47- and 95-fold increase of the drug oral bioavailability and half-life, respectively, with respect to the free unprocessed drug. These results support the outstanding performance of this platform to reduce the dose and the frequency of administration of protease inhibitors, a crucial step to overcome the current patient-incompliant therapy.

© 2014 Elsevier Ltd. All rights reserved.

1. Introduction

The Human Immunodeficiency Virus (HIV) infection is one of the major health burdens worldwide, having claimed approximately 36 million lives since the beginning of the epidemic in the 1980s [1,2]. Chronic administration of a minimum of three antiretrovirals (ARVs) of at least two different families with high frequency is mandatory to maintain undetectable viral levels in plasma over time and to prevent the progress to the active phase of the disease, the Acquired Immunodeficiency Syndrome (AIDS) [3]. Moreover, to achieve therapeutic success, adherence levels need to be at least 95% [4]. On the other hand, complex administration regimens for life jeopardize patient compliance and increase the chances of treatment interruption that results in viral rebound and resistance development. Protease inhibitors (PIs) are a family of ARVs that inhibit the activity of the viral protease, an enzyme that is fundamental for the life cycle of the HIV [5]. PIs are substrates of the P-glycoprotein efflux pump in the intestinal epithelium and the cytochrome P450 metabolic pathway in the liver, two mechanisms that significantly decrease their oral bioavailability [6—8]. To overcome this, they are co-administered with a boosting agent, ritonavir [9—12].

Indinavir (IDV) is a PI that was approved by the US-FDA in 1996 [13]. Due to a very short half-life ($t_{1/2}$, 1—2 h), it is administered thrice a day. Renal adverse effects and the development of viral resistance have relegated it to second-line treatments in developing countries [14]. In this scenario, state-of-the-art PIs that are better tolerated have gained a central role in first-line regimens, as

recently stressed in a multicenter clinical trial conducted in naïve HIV-infected patients [15]. Most of the PIs display very low aqueous solubility, the solubility increasing at low pH to variable extents that depend on the drug. This is why, for example, IDV is commercialized as sulfate, a water-soluble salt of sulfuric acid. Conversely, other protease inhibitors are used as solvates of ethanol (ethanolate), derivatives that increase the aqueous solubility of the drug, though to a much more limited extent (e.g., darunavir). Finally, other PIs are used as free base of very low aqueous solubility (e.g., ritonavir, lopinavir, tipranavir) [16]. Independently of the form used, PIs display very slow dissolution rates in the intestinal medium, a property that contributes to decrease their oral bioavailability [8,17]. In this framework, the development of innovative drug delivery systems (DDSs) that increase the intestinal absorption and decrease the frequency of administration of PIs emerges as a research area of great impact to improve the therapeutic outcomes in HIV [18].

Nanoparticle-in-Microparticle Delivery Systems (NiMDSs) are a DDS formed by drug-loaded nanoparticles that are re-encapsulated within microparticles [19]. The use of mucoadhesive polymers to produce the microparticle component would be advantageous to prolong the residence time of the NiMDS in the gut and increase the oral bioavailability of the encapsulated drug [19,20]. Moreover, the sustainment of the drug release would enable the reduction of the administration frequency.

Aiming to improve the oral bioavailability and reduce the administration frequency of PIs, in this work, we took advantage of the poor aqueous solubility of IDV free base (similar to first-line PIs) and used it as model drug to design a simplified two-components NiMDS. For this, pure IDV free base nanoparticles were produced by nanoprecipitation and encapsulated within mucoadhesive polyelectrolyte complex alginate/chitosan microparticles that were finally film-coated with a mucoadhesive water-insoluble and permeable poly(methacrylate).

2. Materials and methods

2.1. Materials

Indinavir sulfate (Crixivan® 400 mg Capsules; Lot X9308) was a donation of Merck & Co. Inc. (USA). Sodium alginate (Protanal® LF 120 M) was supplied by Productos Destilados SAICyF (Argentina). Chitosan (high viscosity) and chloride calcium dihydrate were purchased from Sigma–Aldrich® (USA) and Anedra® (Argentina) respectively. Eudragit® S100 (an anionic copolymer of methacrylic acid and methyl methacrylate), Eudragit® RL PO (a cationic copolymer of ethyl acrylate, methyl methacrylate and low content of methacrylic acid ester with quaternary ammonium groups) and Eudragit® L100-55 (an anionic copolymer of methacrylic acid and ethyl methacrylate) were kindly donated by Etilfarma® (Argentina). Solvents were of analytical or chromatographic grade.

2.2. Isolation of indinavir free base

IDV free base was isolated from commercial capsules of IDV sulfate, lactose and magnesium stearate employing a methodology described elsewhere with a slight modification [21]. Briefly, the content of 24 capsules was dispersed in distilled water (100 mL) and filtered (Whatman − 1001–500 − Grade 1 Qualitative Filter Paper, Whatman, UK) to remove the water-insoluble magnesium stearate. Then, the resulting solution was alkalinized to pH 6 with NaOH 0.1N to precipitate IDV free base that was extensively rinsed with water to remove residual lactose. Finally, IDV free base was recrystallized from absolute ethanol, dried under vacuum and analyzed to ensure purity. The recrystallization solvent plays a key role in the polymorph formed.

2.3. Production of IDV free base pure nanoparticles

IDV free base nanoparticles were prepared by nanoprecipitation. For this, IDV free base (100 mg) was dissolved in acetone (10 mL, final IDV concentration 1% w/v) and injected into distilled water (400 mL) with a 21G1 needle (internal diameter = 0.80 mm, length = 25 mm) using an infusion pump (flow of 15 mL/h, PC11U, APEMA S.R.L., Argentina) under constant mechanical stirring (700 RPM, IKA Eurostar Digital, Germany), at 19 ± 2 °C. The suspension was stirred for 1 h after the complete addition of the drug organic solution to evaporate acetone, filtered under vacuum (VWR 410 Qualitative Filter Paper, particle retention 2 μm, VWR

International, USA), frozen at −80 °C and lyophilized for 48 h (Freeze Dryer Unit GAMMA A, Christ, Germany). This process was conducted at least six times and yields were calculated as the ratio between the weight of recovered IDV free base nanoparticles and the initial amount of raw drug. Results are expressed as mean ± S.D.

2.4. Characterization of IDV free base pure nanoparticles

2.4.1. Particle size analysis and zeta potential

The size (D_h), size distribution (PDI) and zeta potential (Z-potential) of IDV free base nanoparticles were measured with a Zetasizer Nano-ZS (Malvern Instruments, UK) provided with a He–Ne (633 nm) laser and a digital correlator ZEN3600 using an angle of $\theta = 173°$ to the incident beam, at 25 °C. For this, freeze-dried IDV free base nanoparticles were re-dispersed in 0.1% w/v Tween 80 solution and vortexed for 5 min [22]. Results are expressed as the mean ± S.D. of three samples prepared under identical conditions and each one of them is the result of at least five runs.

2.4.2. Morphology analysis

The morphology of raw and nanonized IDV free base was visualized by SEM (FEG-SEM, Zeiss Supra 40 TM apparatus with Gemini column, Carl Zeiss Microscopy, Germany or Jeol, JSM-6360LV, Japan). Samples were coated with gold by the cathode dispersion method.

2.4.3. Infrared spectroscopy

Infrared analysis of unprocessed and nanonized drug was conducted in a Nicolet Spectrometer (Nicolet 380 ATR/FT-IR spectrometer, Avatar Combination Kit), Smart Multi-Bounce HATR with reflection ATR ZnSe crystal using an angle of 45° (Thermo Scientific, USA) and recorded in a scanning range of 500–4000 cm^{-1}, with resolution of 4 cm^{-1} and 32 scans. Spectra were obtained using the OMNIC 8 spectrum software (Thermo Scientific).

2.4.4. Thermal analysis

IDV free base nanoparticles and raw IDV free base were analyzed by differential scanning calorimetry (DSC, Mettler-Toledo TA-400 differential scanning calorimeter, Mettler-Toledo, USA) and thermogravimetric analysis (TGA, Shimadzu DTG-50 Instrument, Japan). DSC samples (3–5 mg) were sealed in 40 μL Al crucible pans (Mettler ME-27331, Mettler-Toledo GmbH, Switzerland) and heated in a simple heating temperature ramp in the range between 30 and 300 °C, with a heating rate of 10 °C/min under dry nitrogen atmosphere (10 mL/min). TGA samples (3–5 mg) were heated at a rate of 10 °C/min under analytical air.

2.4.5. X-ray diffraction (XRD)

X-ray diffraction patterns of unprocessed and nanonized drug powders were analyzed in an Empyrean Diffractometer (PANalytical, Netherlands) with Ni-filtered Cu radiation generated at 40 mA and 40 kV in the range of 5–40° 2θ with a step size of 0.02° through continuous mode.

2.4.6. Gas Chromatography (GC)

Residual acetone in IDV free base nanoparticles was examined by Gas Chromatography (Hewlett Packard 6890 Gas Chromatograph, Agilent Technologies, USA) equipped with a methyl silicone CBP1-M25-025 fused silica capillary column (25 m × 0.22 mm; film thickness, 0.25 pm). Samples were re-suspended in distilled water (10 mg/mL), vortexed for 10 min and injected (1 mL) into the chromatograph using helium as carrier. The column temperature was maintained at 50 °C, while the temperature of the flame ionization detector and injector were kept at 250 °C. This process was performed in triplicate.

2.4.7. Dissolution

Dissolution profiles of processed and unprocessed drug were evaluated under *sink* conditions using a USP type 2 (paddle) dissolution test apparatus (Alycar Instrumentos, Argentina) [23]. Briefly, an accurately weighed sample (6 mg) was placed in phosphate buffer pH 6.8 (900 mL) used as the dissolution medium. The stirring speed and temperature were maintained at 50 RPM and 37 ± 0.1 °C, respectively. At specific time points (0.75, 1, 2 and 4 h) an aliquot (3 mL) of dissolution medium was withdrawn with media replacement, filtered (0.22 μm nitrocellulose membrane, Osmonics Inc., USA) and analyzed by high performance liquid chromatography (HPLC, see below) following a protocol described elsewhere [22]. Measurements were performed by triplicate and results are expressed as the mean ± S.D. Statistical analysis was conducted with a *t*-test (5% significance level), using GraphPad Prism version 6.00 for Windows (GraphPad Software, Inc., USA).

2.5. Preparation of NiMDSs

IDV free base pure nanoparticles were primarily encapsulated within calcium alginate/chitosan polyelectrolyte complex microparticles. For this, IDV nanoparticles (3.0, 4.5 and 7.5 mg) were suspended in sodium alginate solution (2.4% w/v, 1.5 mL) and injected into a CaCl$_2$/chitosan solution of pH 5.50 (30 mL, final concentrations of 0.1M and 0.2% w/v, respectively) using a 22G1 needle (internal diameter = 0.70 mm, length = 25 mm) and an infusion pump (PC11U, constant flow rate of 40 mL/h) under magnetic stirring (200 RPM). Microparticles were maintained under magnetic

stirring for 1 h after the end of the injection to allow ionotropic crosslinking, filtered (Polypropylene, XN 6070, aperture 0.025 × 0.03 inches, Industrial Netting, USA), extensively rinsed with distilled water to remove non-encapsulated drug, chitosan and $CaCl_2$ residues and dried at room temperature. For film-coating, copolymers were dissolved in absolute ethanol under vigorous magnetic stirring overnight. Then, dry microparticles were pre-hydrated by submerging into pure water under magnetic stirring (100 RPM, 3 min) and filtered by a plastic mesh (see above). Beads were consecutively dipped in a solution of Eudragit® S100 (10% w/v, 3 mL, magnetic stirring of 100 RPM, 30 min) and a solution of Eudragit® RL PO (15% w/v, 3 mL, magnetic stirring of 100 RPM, 30 min). Finally, film-coated microparticles were filtered using a plastic mesh (see above) and dried on Parafilm® at room temperature. The variables tested to optimize the film-coating process are summarized in Table 1. To prepare blank microparticles, the same protocol was followed, though without the addition of IDV. Non-coated NiMDSs were also used along the work to compare with the film-coated counterparts. All experiments were performed in triplicate.

2.6. Characterization of blank microparticles and NiMDSs

2.6.1. Particle size analysis

The size of blank microparticles and NiMDSs was measured by micrometry (M110-25, Mitutoyo, Japan) and optical microscopy (Arcano, China) coupled to a digital camera and TS View Digital imaging software. Results are expressed as the mean ± S.D. of 105 particles obtained in 10 independent batches.

2.6.2. Morphology analysis

The morphology and the topography of uncoated and film-coated NiMDSs were visualized by SEM under the conditions depicted above for pure IDV free base nanoparticles. Uncoated and film-coated blank microparticles were evaluated for comparison.

2.6.3. Drug encapsulation efficiency and drug cargo

The encapsulation efficiency (%EE) and drug cargo (DC) were determined by an indirect method. For this, the $CaCl_2$/chitosan supernatant used to produce NiMDSs and containing non-encapsulated pure IDV nanoparticles in suspension was recovered, lyophilized and dissolved in methanol. The concentration of free IDV (D_f, non-encapsulated drug) was determined by UV spectrophotometry (λ = 261 nm, CARY [1E] UV-Visible Spectrophotometer Varian, USA). The %EE was calculated according to Equation 1.

$$\%EE = \left[\left(D_o - D_f \right) \middle/ D_o \right] \times 100 \qquad (1)$$

and the DC (%) in the NiMDSs was calculated according to Equation 2.

$$DC(\%) = \left[\left(D_o - D_f \right) \middle/ P \right] \times 100 \qquad (2)$$

where D_o is the initial amount of IDV used in the production of NiMDSs, D_f is the amount of non-encapsulated IDV determined in the $CaCl_2$/chitosan supernatant and P is the weight of the NiMDSs in each specific batch. Results are expressed as mean ± S.D. (n = 3).

2.6.4. Coating thickness

The size of 20 uncoated and film-coated blank microparticles from three independent batches was determined by micrometry (see above). The average film thickness for each microparticle was estimated by subtracting the mean size of the uncoated microparticles from the mean size of the film-coated ones. Additionally, a defined amount of microparticles (20 mg) was weighed before and after coating to determine the weight of coating added to the microparticles (m_{ca}, expressed as %) according to Equation 3.

$$m_{ca} = [(m_c - m_u)/m_u] \times 100 \qquad (3)$$

where m_c and m_u are the mass of the microparticles after and before the film-coating, respectively.

Table 1
Optimization of the microparticle film-coating conditions.

Sample	Hydration prior to coating	Coating layers	Layer composition
DM	No	1 (Monolayer)	Eudragit® RL
HM	Yes	1 (Monolayer)	Eudragit® RL
HB	Yes	2 (Bilayer)	Inner layer, Eudragit® S100 Outer layer, Eudragit® RL

DM: Dry monolayer.
HM: Hydrated monolayer.
HB: Hydrated bilayer.

2.6.5. Swelling

The swelling was assessed by gravimetry. Dried microparticles (n = 10) were accurately weighed and immersed in phosphate buffer of pH 6.8, at 37 ± 1 °C. At predetermined time points, microparticles were filtered using a plastic mesh (see above) and carefully wiped with tissue paper before weighing them again. The degree of swelling (Q_t) was calculated according to Equation 4.

$$Q_t = [(W_t - W_o)/W_o] \times 100 \qquad (4)$$

where W_t is the weight of the swollen microparticles at a time t and W_o is the initial weight of the dry microparticles. Results are expressed as mean ± S.D. (n = 3).

2.7. Mucoadhesion ex vivo

Mucoadhesion of microparticles was conducted *ex vivo* using a USP type 2 dissolution test apparatus. In brief, a piece of fresh bovine gut (2 cm × 4 cm) was rinsed and hydrated with distilled water and attached to a microscope glass slide. Then, uncoated or film-coated blank microparticles (n = 10) were randomly dispersed onto the piece of mucosa, immersed in phosphate buffer of pH 6.8 (500 mL) at 37 ± 0.1 °C, mechanically stirred (25 RPM) and the number of microparticles that remained adhered to the mucosa quantified every hour for a lapse of 6 h. To ease the visualization of the microparticles in the tissue, Bright Blue dye was added to the $CaCl_2$ crosslinking solution at a final concentration of 0.025% w/v. Then, the percentage of remaining microparticles at each time point was calculated according to Equation 5.

$$\text{Percentage of adhered NiMDSs} = [n_t/n_o] \times 100 \qquad (5)$$

where n_t is the number of microparticles that remained adhered at time t and n_o is the initial number of microparticles, namely 10. All the assays were performed in triplicate and results are expressed as mean ± S.D.

2.8. Drug release in vitro

The release of IDV from NiMDSs with different cargos was conducted in phosphate buffer pH 6.8 (10 mL) containing 0.5% w/v Tween® 80, at 37 ± 2 °C. For this, NiMDSs containing 1.5 mg of IDV free base nanocrystals were immersed in the release medium and magnetically stirred for 8 h. The surfactant was added to increase the intrinsic solubility of the drug in the release medium and to prevent adsorption of the drug on the surface of the container [24]. At predetermined time points, three aliquots (2—3 mL each) were withdrawn and the medium was replaced by fresh pre-heated medium. Medium exchanges also ensured the maintenance of *sink* conditions [23,25]. The first aliquot was filtered (0.45 μm nitrocellulose membrane, Osmonics Inc., USA) to remove IDV nanocrystals (insoluble drug) and the concentration of soluble IDV quantified by HPLC (see below). The second aliquot was diluted with acetonitrile (1:1), vortexed for 1 min and filtered (0.45 μm nylon membrane, MSI, USA). Then, the filtrate was analyzed by HPLC (see below) to quantify the total amount of released drug (nanocrystals + soluble drug). Finally, the third aliquot was used to analyze the size and size distribution of the nanocrystals by DLS (see above). All experiments were carried out in triplicate and results are expressed as mean ± S.D. To evaluate the release mechanism, data were fitted to Higuchi and Korsmeyer-Peppas models using Microsoft® Excel 2010 and SigmaPlot® 12.0 Software, respectively.

2.9. Pharmacokinetic studies

2.9.1. Preparation of enteric capsules loaded with IDV

Capsules number 1 (length = ~19 mm) were loaded with (i) unprocessed IDV free base (control), (ii) pure IDV free base nanoparticles and (iii) film-coated NiMDSs [26]; capsules were prepared individually and the IDV cargo adjusted to the weight recorded for each mongrel dog according to a dose of 10 mg/kg (see below). To confer gastro-resistance, capsules loaded with the different samples were subjected to a film-coating process by individually immersing them in Eudragit® L100-55 ethanol solution (10% w/v, 5 min) and drying by convection, alternating cold and warm air [27]; the process was repeated five times. To assess the efficiency of the coating, a disintegration test was carried out at 37 ± 2 °C [28]. Briefly, each coated capsule (n = 6) was individually placed in the basket of a Disintegration Test Apparatus (Hally Instruments, India), the disintegration medium was added (900 mL) and the basket-rack was subjected to vertical movements (29—32 cycles/min). The assay was performed in 0.1 N HCl solution for 2 h and in phosphate buffer (pH 6.8) for one additional h. At the end of each time point, the integrity of every capsule was visually examined.

2.9.2. Oral bioavailability assays

Oral bioavailability assays were performed in mongrel dogs (n = 4, weight of 10.8 ± 4.1 kg) according to the Directive 2010/63/EU on the protection of animals used for scientific purposes (22 September 2010, European Union). This animal model was selected based on its ability to swallow the gastro-resistant capsule loaded with the different samples. The preclinical protocol was approved by the Animal Welfare Committee of the Faculty of Veterinary Sciences (Resolution #28/2013, National University of Central Buenos Aires, Argentina). Animals were fasted

overnight prior to the administration of the corresponding capsule and fed 3—4 h after the administration. At predetermined time points post-administration, blood samples were extracted (3 mL) [29] and immediately centrifuged (2500 RPM) to separate plasma that was frozen at −20 °C until analysis.

2.9.3. Plasma analysis

A validated method already reported with a slight modification was used to quantify the drug in plasma [30]. For this, samples were thawed and vortexed for 10 s. Then, NaOH 1M (100 μL) and ethyl ether (5 mL) were added to plasma (1 mL) and the mixture hand-shaken (4 min) to extract IDV to the organic phase and re-frozen at −20 °C to separate it from the aqueous one. Organic solutions were dried in a water bath at 35 °C and atmospheric pressure and the residue was reconstituted in HPLC mobile phase (1 mL, see below), filtered (0.45 μm nylon membrane, MSI) and analyzed (see below). The following pharmacokinetic parameters were calculated using a non-compartmental model (TOPFIT program version 2.0, Dr. Karl Thomae Gmbh, Schering AG, Germany): (i) maximum plasma concentration (C_{max}), (ii) time to C_{max} (t_{max}), (iii) the area-under-the-curve between 0 and 4 h (AUC_{0-4}), (iv) the area-under-the-curve between 0 and ∞ ($AUC_{0-\infty}$) and (v) apparent half-life in plasma ($t_{1/2}$). The relative oral bioavailability was calculated according to Equation 6.

$$F_r = AUC_S/AUC_R \qquad (6)$$

where AUC_S and AUC_R are the $AUC_{0-\infty}$ of each sample and of unprocessed IDV (control), respectively.

Results are expressed as mean ± coefficient of variation (CV%). Differences among groups were analyzed using one-way analysis of variance (ANOVA, significance level of 5%) with Bonferroni test.

2.9.4. HPLC method

HPLC analysis was conducted using an Alliance separation module e2695 (Waters Corp., USA) equipped with an Eurospher II C18P column (5 mm, 150 × 4 mm, Knauer, Germany) and a UV detector (2998 Photoiodide Array UV/Vis 2D detector, W2998, Waters Corp., USA). Measurements were performed at 25 °C using an isocratic flow of 1 mL/min. The injection volume was 100 μL and the detection was performed at λ of 210 nm. The mobile phase employed was acetonitrile:triethylammonium buffer (pH 6.5) in a volume ratio of 37:63 for plasma analysis and 40:60 for measurement of IDV concentration in release and dissolution assays. The former was validated over the range of 0.02—5 μg/mL ($R^2 > 0.999$) and the latter in the range of 0.05—20 μg/mL ($R^2 > 0.998$). In both cases within- and between-day precision analyses were always less than 10% for all quality control samples.

3. Results and discussion

3.1. Rationale

Due to the serious biopharmaceutical drawbacks of PIs, the design of innovative DDSs that improve their oral bioavailability and prolong their $t_{1/2}$ is urgently called for. In this study, we used IDV as a versatile model PI and develop a drug delivery platform that would not only sustain its release over time but that could be also extended to newer PIs with minor adjustments. In this framework, the use of IDV free base (and not of the water-soluble sulfate), a derivative of very low aqueous solubility in the intestinal medium as most of the state-of-the-art PIs, including the latest and most effective darunavir, was more appropriate. Thus, the rationale was to nanonize IDV free base (model drug) to increase the surface area and thus the dissolution rate (and the oral bioavailability). Then, encapsulation of these nanoparticles within mucoadhesive microparticles that adhere to the intestinal mucosa would control and prolong the release of the encapsulated drug. To minimize the release of IDV in the stomach, NiMDSs were re-encapsulated within gastro-resistant capsules that would undergo fast disintegration only in the intestinal medium, releasing the DDS exclusively at the absorption site (Fig. 1).

3.2. Production and characterization of IDV free base nanoparticles

Pure drug nanoparticles emerge as a simple and straightforward approach for enhancing the dissolution rate of poorly water-soluble drug like PIs [31,32]. Nanoprecipitation was selected to produce the drug nanoparticles because it is simple, economic, and reproducible and with relatively high yield [33]. Acetone was used as the solvent because it dissolves efficiently the drug, is miscible with the anti-solvent (water) and is classified into Class III (solvents with low toxic potential) by the International Conference on Harmonization (ICH) guidelines [34]. Furthermore, it can be effectively extracted by evaporation under normal pressure over a short time. The production yield was 70.1 ± 5.0%, the remaining 30% being retained by the filter paper due to a particle size that was larger than the filter pores (2 μm). IDV free base nanoparticles showed a size of 724 ± 61 nm with a relatively low PDI value of 0.143 ± 0.079 (as measured by DLS). SEM analysis confirmed the sharp reduction of the particle size with respect to unprocessed IDV and evidenced the irregular morphology of the pure drug nanoparticles (Fig. 2). The Z-potential of IDV free base nanoparticles was −16.7 ± 0.32 mV. This result did not stem from the anionic nature of IDV free base but
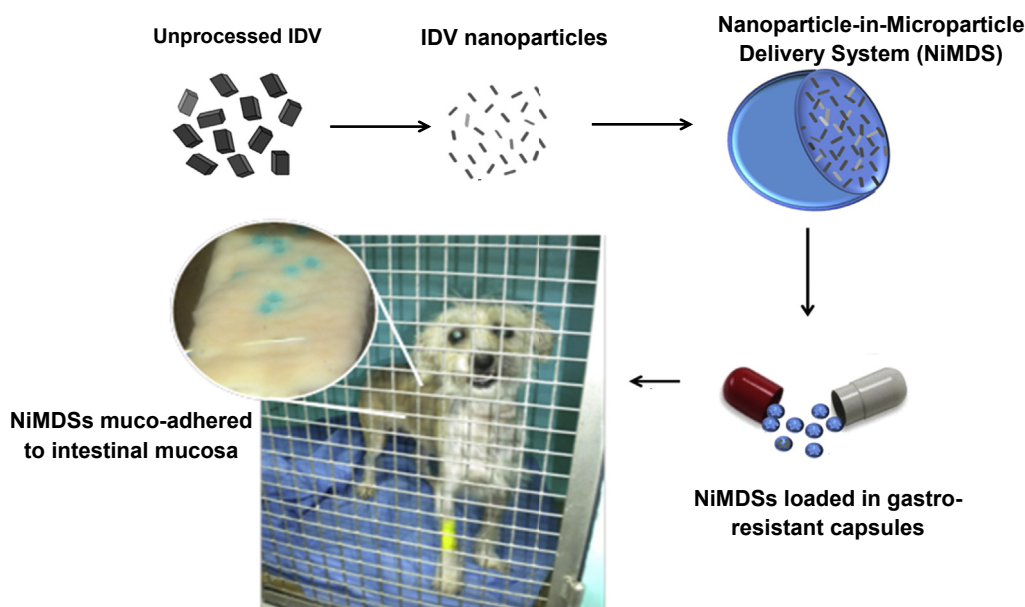

Fig. 1. Design rationale of IDV free base-loaded NiMDSs. NiMDSs were re-encapsulated within gastro-resistant capsules that underwent fast disintegration only under intestinal pH conditions, releasing the DDS exclusively at the absorption site (gut).

most probably from the polarization of amide groups on the surface of the crystals, where the oxygen atom bears a negative charge density. A similar phenomenon was previously reported for pure nanoparticles thiosemicarbazones of 1-indanone [35].

ATR/FT-IR analysis showed that the characteristic peaks of IDV were conserved in the nanoparticles, confirming that the processing method did not affect the integrity of the drug (Table 2). However, small shifts in the bands of IDV nanoparticles with respect to the unprocessed drug suggested small changes in the crystalline structure that could be related to the formation of a different polymorph or pseudo-polymorph [22].

Complementary thermal analysis also revealed changes after the processing of the drug. The DSC thermogram of unprocessed IDV free base showed two endotherms. The first weak and sharp endotherm at 130 °C corresponded to the release of one molecule of water bounded to the crystal lattice [22], as confirmed by TGA that showed 2.4% weight loss. The second strong endotherm at 152 °C ($\Delta H_m = 58$ J/g) corresponded to the T_m of the drug. The thermal behavior of IDV nanoparticles was different with a small broad endotherm at 108 °C that was attributed to the loss of free water (2.7% w/w weight loss that corresponded to one molecule of water, as measured by TGA) and a second endothermic peak at 146 °C ($\Delta H_m = 53$ J/g) due to the melting of the drug. Differences between the T_m values of the unprocessed and nanonized drug (152 and 146 °C, respectively) would stem from the presence of water molecules bounded to IDV with different strength and the alteration of the forces in the crystal lattice to some extent. In fact, water-drug bonds can alter the cooperativity of the molecules in the crystal lattice and thus the T_m [36]. These findings would be in agreement with the formation of different pseudo-polymorphs. At the same time, the energy involved in the melting was very similar for both products.

XRD analysis showed similar diffraction patterns for both the unprocessed and the nanonized drug, with characteristic peaks in 2θ 6.53°, 7.85°, 10.29°, 13.02°, 13.63°, 15.28°, 15.81°, 17.09°, 17.78°, 20.61°, 21.27°, 23.08°, 23.76°, 26.34°, 28.10°, 29.07°, 29.96°, 31.03°, 32.48°, 33.11°, 33.40°, 34.08° and 35.34° (Fig. 3). However, some changes in the relative intensity of the peaks were apparent in IDV nanoparticles [22]. Overall data of ATR/FT-IR, thermal analysis and XRD indicated that raw and nanonized IDV free base have the same internal crystalline structure and that they would be two different pseudo-polymorphs.

As expected, the dissolution test of the unprocessed and processed drug showed a statistically significant increase of the dissolution rate upon nanonization (Fig. 4). For example, after 45 min and 4 h, 17% and 42% of raw IDV free base underwent dissolution, respectively. Conversely, for the nanoparticles, values

Table 2
ATR/FT-IR of unprocessed and nanonized IDV free base.

Unprocessed IDV	IDV nanoparticles	Assignment
3486	3504	N—H stretching vibration of piperazine
3349	3441	N—H stretching vibration of amide
3283	3297	O—H stretching
2950	2949	C—H stretching in aliphatic
1732	1731	C=O stretching
1653, 1636	1657, 1642	C=O stretching vibration of amide
1540, 1523	1549, 1526	C=C stretching in aromatic
1456	1454	Interaction between ring C—C and C—N stretching vibration in pyridine
1362, 1151	1363, 1153	C—O stretching and O—H bending vibration of secondary alcohol
701, 752	705, 753	C—H stretching in aromatic ring

were 32% and 69%. These results were in accordance with data reported elsewhere [22] and were envisioned to have a strong impact on the oral bioavailability of IDV, as they took place within a time range that fitted well the intestinal transit.

Nanoprecipitation employed acetone, a solvent that needs to be effectively eliminated to prevent any toxic effects during the preclinical evaluation of the systems. GC analysis revealed the absence of solvent traces in all the samples.

3.3. Production and characterization of NiMDSs

Aiming to modulate the release and increase the residence time of the drug in the bowel, IDV free base nanoparticles were encapsulated within mucoadhesive microparticles. Alginate and chitosan are natural mucoadhesive polysaccharides obtained from the cell walls of brown algae and the shell of crustaceans, respectively [20,37,38]. Due to low toxicity, good biocompatibility and biodegradability they have been extensively investigated for the development of pharmaceuticals and have been listed as "Generally Referred as Safe" (GRAS) by the US-FDA [20]. Alginate is a polyanion that undergoes ionotropic gelation with calcium ions and chitosan, a polycation. Thus, their combination gives place to relatively stable polyelectrolyte complex matrices. According to this, microparticles were initially produced by polyionic complexation between sodium alginate, calcium ions and chitosan. However, it is noteworthy that a pH value greater than 6 (as in the intestinal medium) leads to deprotonation of the amine groups of chitosan and the weakening of the electrostatic forces with alginate, increasing the swelling and favoring fast matrix disintegration [39,40]. Similarly, the chelating action of phosphate anions in the gastrointestinal medium results in the exchange of calcium in the network by sodium, a process that
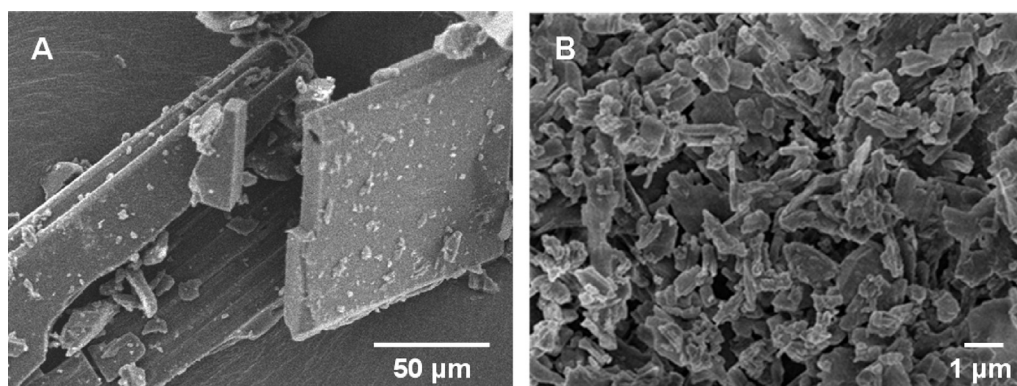

Fig. 2. SEM micrographs of (A) unprocessed IDV free base and (B) IDV free base nanoparticles produced by nanoprecipitation from acetone. Scale bar: (A) = 50 μm, (B) = 1 μm.
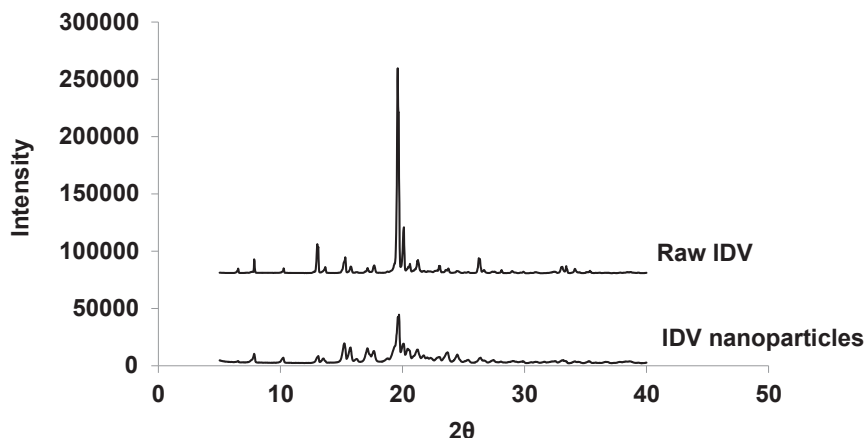
Fig. 3. XRD pattern of IDV free base before (raw IDV) and after nanonization (IDV nanoparticles).

destabilizes the complex and also promotes matrix disintegration [41].

Swelling plays a fundamental role in the physical stability of polymeric matrices and the release rate of encapsulated drugs; the greater the swelling, the faster the disintegration and the release. Since NiMDSs are expected to remain adhered to the intestinal mucosa and prolong the release of IDV, swelling was initially assessed and the composition of the microparticles adjusted to minimize this phenomenon. Regardless of the mechanisms, un-coated microparticles underwent fast swelling (3600% in 2 h) and disintegration in medium of intestinal pH (Fig. 5). This process was undesired because it would be associated with the fast release and dissolution of the microencapsulated IDV nanoparticles. To mini-mize and delay swelling, microparticles were film-coated with a series of water-insoluble copolymers that are commonly used for the coating of oral formulations with modified release kinetics. Ethanol was used as solvent because it dissolves very well the coating agents, though it does not dissolve the drug cargo. Eudra-git® RL was selected to film-coat the microparticles because it is water-insoluble and water permeable, enabling the slow diffusion of encapsulated drugs. An additional appealing feature of this copolymer is the presence of quaternary ammonium groups that confer mucoadhesiveness owing to their ability to electrostatically interact with mucin, the main component of the intestinal mucosa [42,43]. Initially, dry chitosan/alginate microparticles were film-coated with a monolayer of Eudragit® RL (DM microparticles, Table 1). The coating reduced the swelling of the microparticles from 3600% to less than 2000% (Fig. 5). However, they disintegrated within 2 h. To improve the integration of the coating to the mi-croparticles by means of polymer chain interpenetration, a hydra-tion step was introduced before the film-coating. This modification was reflected by a slight decrease of the swelling and a substantial increase of the physical stability (HM microparticles, Fig. 5). Finally, to further improve the integration of the Eudragit® RL outer coating, an intermediate coating of Eudragit® S100 was performed. This copolymer is polyanionic and it would undergo electrostatic interaction with both the positively-charged surface of the micro-particles (owing to the excess of chitosan used in the crosslinking
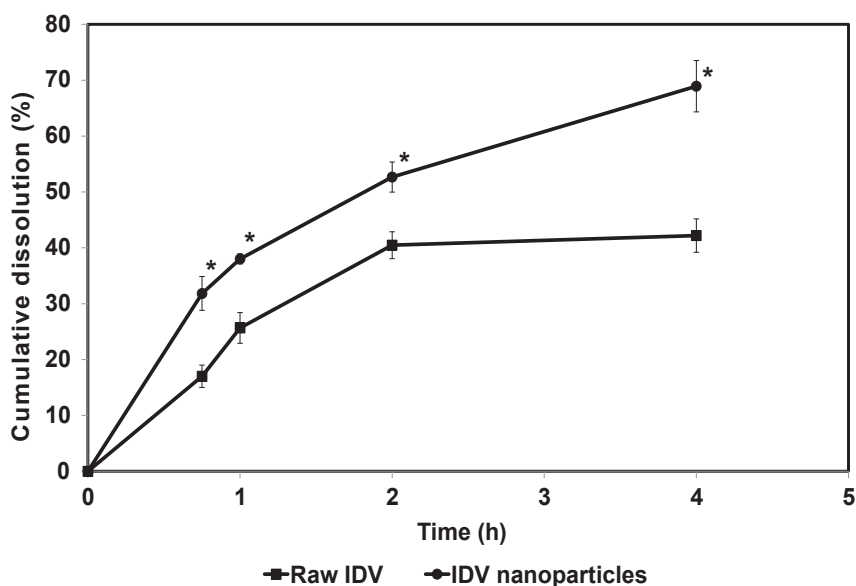

Fig. 4. Cumulative dissolution of unprocessed IDV free base (■) and pure IDV free base nanoparticles (●) in PBS of pH 6.8, at 37 °C. The dissolution was assessed under intestinal pH conditions because the NiMDSs were re-encapsulated within gastro-resistant capsules that disintegrate exclusively in the gut. *Statistically significant increase of the amount of drug dissolved when compared to unprocessed IDV ($p < 0.05$).
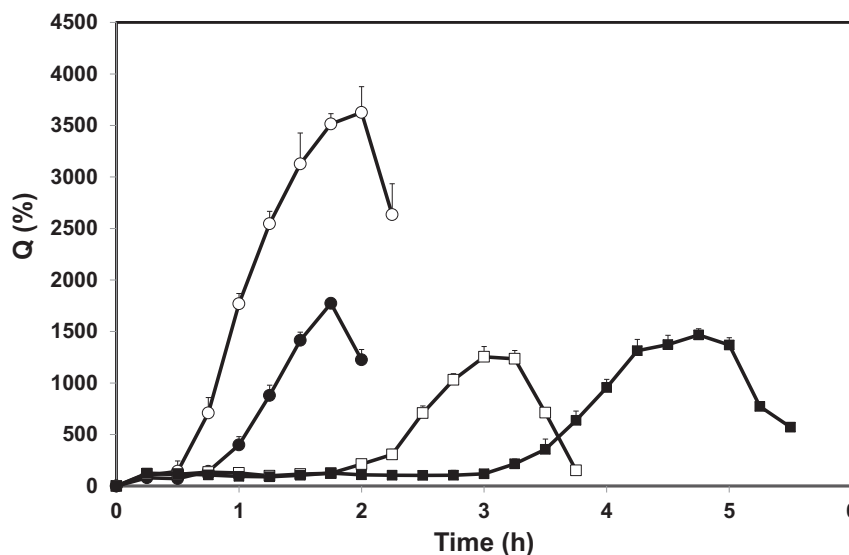
Fig. 5. Swelling profile of uncoated microparticles (○), film-coated with a monolayer of Eudragit® RL without (DM, ●) and with (HM, □) pre-hydration step and film-coated microparticles with a polymeric bilayer (HB, ■), in phosphate buffer of pH 6.8 at 37 °C.

solution) and with the electropositive copolymer (Eudragit® RL) used to form the outer layer (HB microparticles, Fig. 5). This film-coating reduced the maximum swelling extent to 1460% and delayed the beginning of the disintegration *in vitro* to 5 h (Fig. 5), a time that fits the gastrointestinal transit and that would favor the adhesion of the DDS to the intestinal mucosa. Furthermore, late microparticle disintegration would be beneficial to promote the entrapment of IDV nanoparticles in the mucosa and a prolongation of their residence time and release. Based on these results, different cargos of IDV free base nanoparticles were homogeneously dispersed in the alginate precursor solution and then, microparticles produced and film-coated with a bilayer. In all cases, %EE was almost 100% and the drug cargo up to 43% based on dry weight (Table 3). The morphology and the topography of uncoated and coated NiMDSs containing growing IDV cargos were analyzed by SEM. Before film-coating, microparticles displayed a rough and porous surface characteristic of dry polysaccharide matrices (Fig. 6A,C,E,G). In addition, when IDV nanoparticles were incorporated, the porosity increased (Fig. 6C,E,G). This structure would favor the fast release of superficial drug by means of dissolution and desorption of whole nanoparticles. Conversely, upon film-coating, the surface of the microparticles became very smooth and deprived of cracks. To rule out the dissolution of IDV nanoparticles during the coating process, the drug concentration in the different ethanol solutions used was determined by HPLC; IDV could not be detected. The contribution of the bilayer film-coating to the thickness and the weight of the microparticles was evaluated by

micrometry and gravimetry. The average film thickness was approximately 40 μm and the size of the microparticles increased from 860 to 900 μm. Furthermore, the weight of the microparticles increased by 20%. This result was in agreement with the literature [44].

3.4. Mucoadhesion

Mucoadhesive polymers can prolong the residence time of the drug-loaded delivery system in the intestine, a phenomenon that usually leads to a sharp increase of the absorption extent and the oral bioavailability [45]. All the components of the microparticle matrix are mucoadhesive by means of different mechanisms [20]. Thus, even after partial or complete disintegration, NiMDSs were expected to remain adhered to mucosa. The mucoadhesion was assessed employing an *ex vivo* test that showed a significant increase of the residence time due to film-coating (Fig. 7). For example, after 6 h, 40% of the film-coated NiMDSs remained adhered, as opposed to 0% of the uncoated counterparts due to fast disintegration.

3.5. IDV release in vitro

Drug release is a complex phenomenon in which several mechanisms may be simultaneously involved [46]. To study the release kinetics of IDV from NiMDSs containing different drug cargos, samples were incubated in PBS of pH 6.8 containing 0.5% w/v Tween® 80 over 8 h. As previously detailed, the surfactant was aimed to increase the aqueous solubility of IDV in the release medium and ensure *sink* conditions. The time of the study was chosen based on the gastrointestinal transit of standard formulations. Moreover, the use of intestinal-like pH medium relied on the fact that re-encapsulation of NiMDSs within gastro-resistant capsules would prevent the fast disintegration and dissolution in an inappropriate body site (stomach) and their direct contact with the gastric medium, and ensure their immediate release once in the gut for IDV absorption.

Irrespective of the cargo, the release showed two well-differentiated phases (Fig. 8). The initial phase was characterized by a slow release, confirming the absence of strong burst effect. This

Table 3
Encapsulation efficiency (%EE) of IDV nanoparticles within alginate/chitosan microparticles.

Sample	Concentration of nanoparticles in alginate solution (% w/v)[a]	Polymer:IDV ratio (w/w)	Drug loading (% w/w)[b]	%EE (%) (±S.D.)
NiMDS-15	0.7	1:0.3	15.1	95.4 (0.6)
NiMDS-28	1.3	1:0.5	27.9	96.2 (0.2)
NiMDS-43	2.7	1:1.1	43.3	98.2 (0.2)

[a] The concentration of sodium alginate was 2.4% w/v.
[b] IDV cargo in dry NiMDSs expressed as % w/w determined before film-coating.
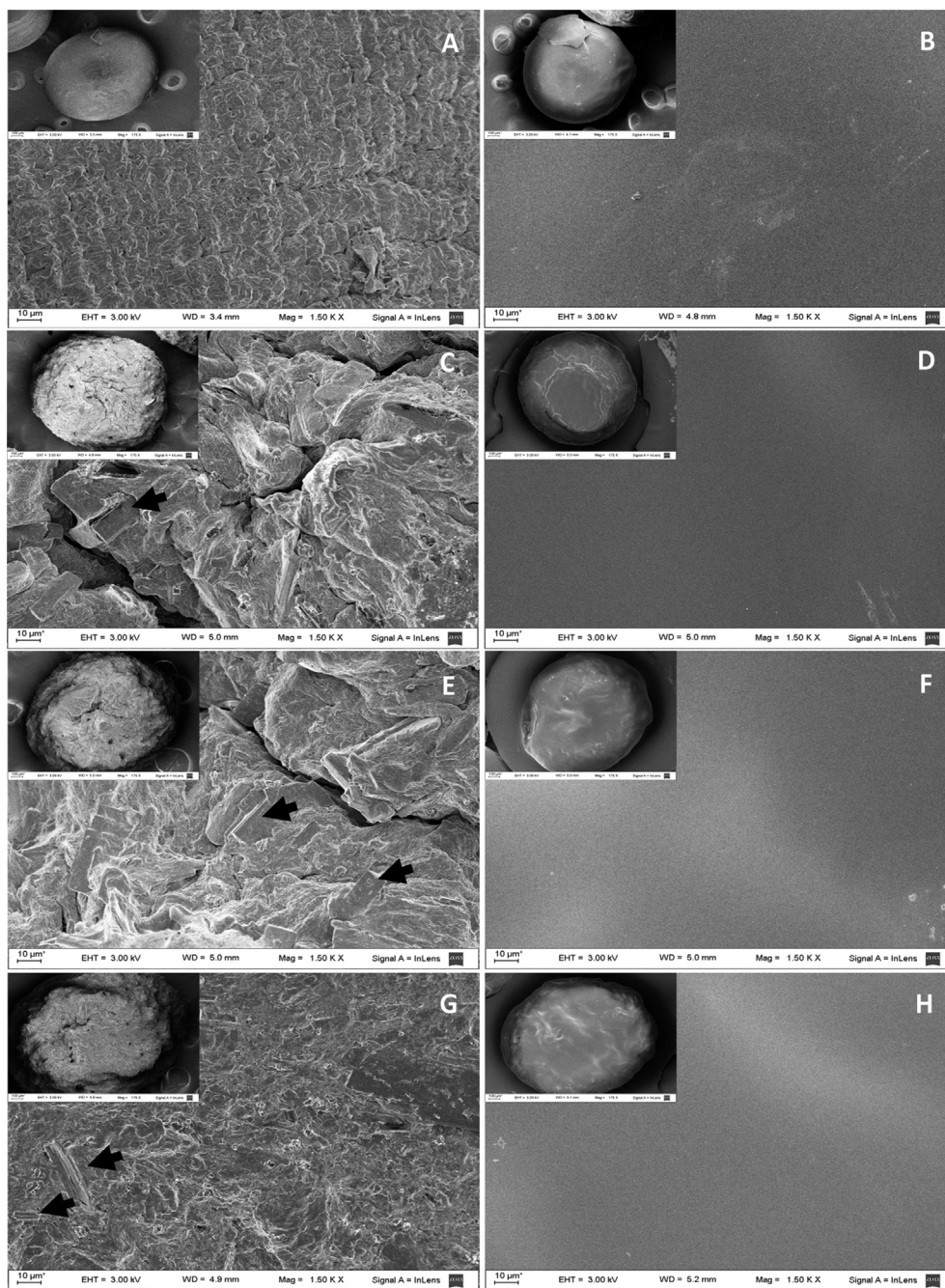
Fig. 6. SEM micrographs of blank microparticles and NiMDSs. (A) Blank microparticles, (B) film-coated blank microparticles, (C) NiMDS-15, (D) film-coated NiMDS-15, (E) NiMDS-28, (F) film-coated NiMDS-28, (G) NiMDS-43 and (H) film-coated NiMDS-43. Insets show the complete microparticle, while the main image the surface of the microparticle. Arrows show the presence of pure IDV free base nanoparticles clusters on the surface of uncoated microparticles. Scale bar: Main image = 10 μm; inset = 100 μm.

behavior stemmed from the relatively slow swelling and the conserved physical integrity of the matrices attained by the bilayer film-coating. Conversely, uncoated NiMDSs released the encapsulated drug very fast (data not shown). Then, an increase of the release rate was observed owing to the swelling and later disintegration of the NiMDSs. In the first phase, both curves overlapped because the low amount of drug that was released underwent dissolution in the release medium. In the second phase, the drug began to be released also in the form of nanocrystals, probably as result of both the relaxation of the polymer chains with the increase of the matrix porosity and due the very low solubility of IDV free base in neutral aqueous medium (pH 6.8).

The release of IDV nanoparticles was confirmed with an additional study conducted by DLS; nanocrystals showed a slight size decrease (542—630 nm) with respect to the original ones, probably due to partial dissolution. This phenomenon would entail an additional advantage because the entrapment of free nanoparticles in the intestinal mucosa would lead to the generation of a drug reservoir that prolongs the release in the absorption site, beyond the residence time of the mucoadhesive microparticles and regardless of their integrity.

To gain further understanding of the mechanisms that control the release, data of the second release phase were fitted to the Korsmeyer-Peppas model according to Equation 7.
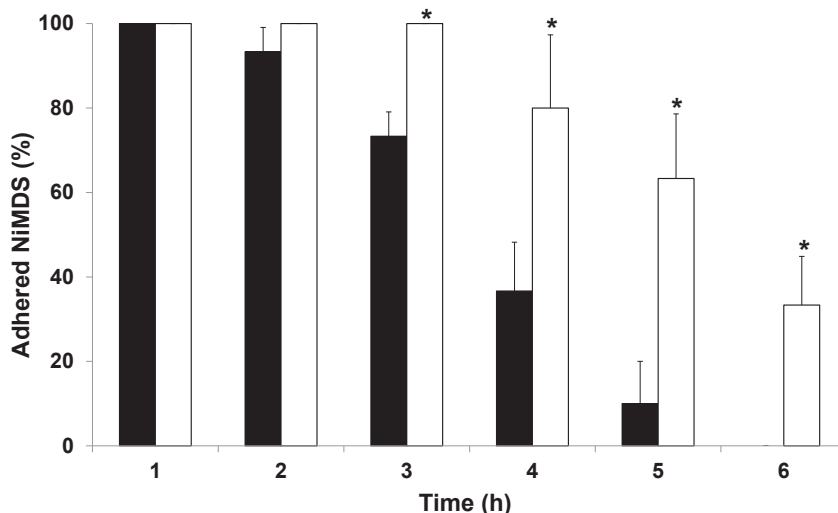
Fig. 7. Percent of uncoated (■) and film-coated NiMDSs (□) adhered to fresh bovine intestine as a function of time. *Statistically significant increase in the percentage of film-coated NiMDSs adhered to the intestinal mucosa with respect to uncoated NiMDSs ($p < 0.05$).

$$Q_t/Q_\infty = k \times t^n \qquad (7)$$

where Q_t/Q_∞ is the fraction of drug released at time t, k is a kinetic constant that reflects the structural and geometric characteristics of the DDS and n is an exponent that provides information about the mechanism of release. For spherical systems (such as NiMDSs), values smaller than 0.43 indicate that the release is controlled by Fickian diffusion, values between 0.43 and 0.85 reveal a non-Fickian diffusion known as anomalous transport which combines diffusion and polymer chain relaxation and values higher than 0.85

indicate that the release is governed exclusively by polymeric relaxation (super case II transport) [47]. All the systems showed n values greater than 0.85, revealing that polymeric relaxation due to matrix swelling was the mechanism governing the release; R^2_{adj} was 0.99, 0.99 and 0.98 for NiMDS-15, NiMDS-28 and NiMDS-43, respectively. Finally, the incorporation of the highly hydrophobic IDV free base reduced the capacity of the microparticles to swell, resulting in a gradual decrease of the release amounts with the increase of the drug cargo. Based on these results, NiMDS-28 were selected to comparatively assess the oral pharmacokinetics of IDV.
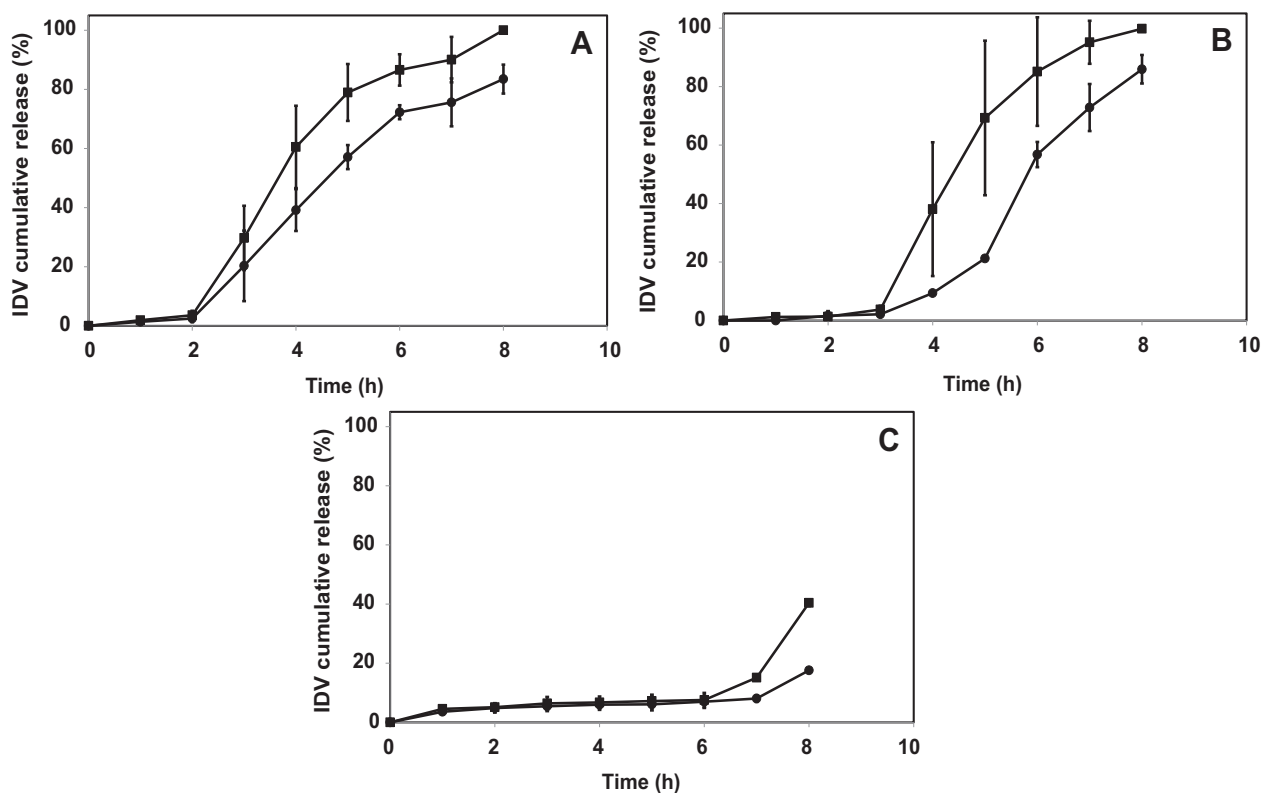

Fig. 8. Release profile of IDV from film-coated (A) NiMDS-15, (B) NiMDS-28 and (C) NiMDS-43 in PBS of pH 6.8 containing 0.5% w/v Tween® 80. (●) Soluble IDV free base and (■) total IDV free base (soluble IDV + nanocrystals).

3.6. IDV oral pharmacokinetics

In vivo studies are critical to evaluate the robustness of the DDS design. Since NiMDSs were re-encapsulated within gastro-resistant capsules, this study was conducted in mongrel dogs that could swallow them. To ensure that the capsules withstand the gastric medium and disintegrate immediately upon contact with the intestinal one, a standardized disintegration test was conducted. Results confirmed the resistance of 100% of the capsules in medium of gastric pH and their fast disintegration (approximately 30 s) in intestinal-like one. Then, a single dose of 10 mg/kg of raw IDV free base, pure IDV nanoparticles and NiMDSs (all of them encapsulated within gastro-resistant capsules) was administered and the concentration of IDV in plasma monitored over time (Fig. 9). The unprocessed drug showed a pharmacokinetic profile that was similar to the one reported in literature [48] with a fast absorption ($t_{max} = 1.10$ h), a relatively low $AUC_{0-\infty}$ of 0.83 μg/mL/h and a fast clearance expressed by a short $t_{1/2}$ of 0.8 h (Table 4). In addition, plasma concentrations were within the therapeutic window defined in humans [48]. Drug nanonization resulted in a dramatic increase of the absorption extent due to the growth of the surface area and the dissolution rate and a longer t_{max} (2.50 h) that strongly suggested the retention of the nanoparticles in the intestinal mucosa by physical entrapment. This hypothesis was supported by the fact that IDV was detected in plasma even at a time point of 24 h that was far beyond its $t_{1/2}$. Conversely, at 48 h, IDV could not be detected. This behavior led to a statistically significant increase of the $AUC_{0-\infty}$ to 18.16 μg/mL/h, that represented an improvement of 21.9 and 27.5 times of the relative bioavailability (F_r) and the apparent $t_{1/2}$, respectively (Table 4). Film-coated NiMDS-28 performed dramatically better than the free drug (regardless of the form) with $AUC_{0-\infty}$ and $t_{1/2}$ values of 39.23 μg/mL/h and 76.3 h, respectively. This represented an increase of the oral bioavailability and the apparent $t_{1/2}$ of 47 and 95 times, respectively, when compared to the unprocessed drug. Moreover, constant plasma concentrations were achieved for at least 48 h. Overall, this pharmacokinetic profile suggested that the oral bioavailability is controlled by three factors: (i) the fraction of drug that undergoes fast dissolution and absorption, (ii) the mucoadhesiveness of the microparticles that prolongs the residence time of the DSS in the gut and thus increases the absorption extent and (iii) the physical retention of pure drug nanoparticles in the mucosa that further prolongs the dissolution of the drug over time. Another outstanding advantage of the NiMDS was the complete prevention of the burst peak shown by free IDV nanoparticles that is usually associated with adverse effects; in this regard, the sharp decrease of AUC_{0-4} from 2.93 to 1.40 μg/mL/h upon microencapsulation was remarkable (Table 4). Interestingly, the apparent t_{max} with NiMDS-28 was attained at a much earlier time (1.8 h) than the lag time for the release of IDV *in vitro* (3 h) (Fig. 8). This result supports the difficulty of predicting the performance of DDS and the relevance of conduction *in vivo* studies. On the other hand, they remain a very valuable tool to adjust the composition and the structure of the DDS and to evaluate parameters such as reproducibility and scalability.

4. Conclusions

The present work reported on the successful production of an innovative DDS composed of pure IDV free base nanoparticles encapsulated within film-coated calcium alginate/chitosan microparticles. Encapsulation of cargos as high as 43% w/w within the mucoadhesive microcarrier was achieved with almost 100% efficiency. Due to the increase of the surface area, nanonized IDV showed a significant increase of the oral bioavailability with respect to the unprocessed drug. In addition, detectable levels in plasma until 24 h suggested that nanoparticles were retained in the
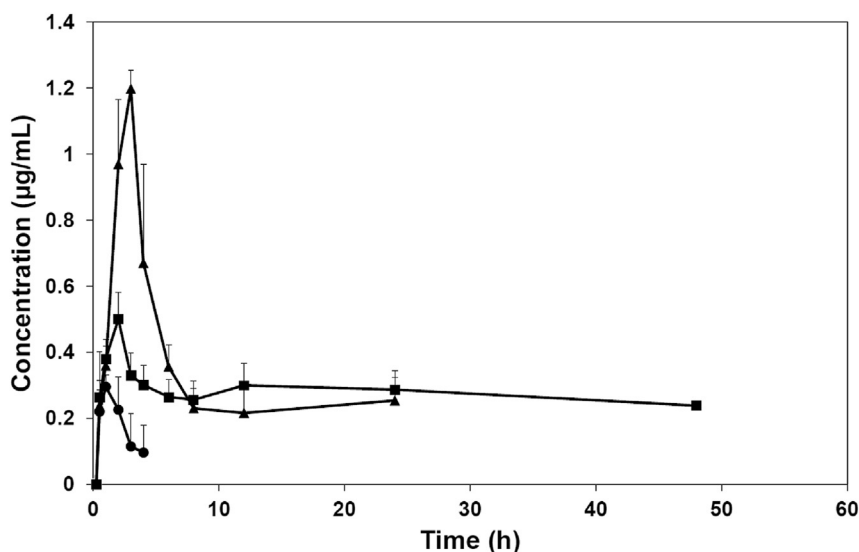
Table 4
Pharmacokinetics parameters after oral administration of a single dose (10 mg/kg) of unprocessed IDV free base, IDV free base nanoparticles and film-coated NiMDS-28 encapsulated within gastro-resistant capsules to mongrel dogs ($n = 4$).

Pharmacokinetic parameter	Unprocessed IDV free base		IDV nanoparticles		Film-coated NiMDS-28	
	Mean	CV (%)	Mean	CV (%)	Mean	CV (%)
C_{max} (μg/mL)	0.34	8	1.41[a]	69	0.50	32
t_{max} (h)	1.10	–	2.00	–	1.80	–
AUC_{0-4} (μg/mL/h)	0.75	62	2.93[a]	26	1.40	25
$AUC_{0-\infty}$ (μg/mL/h)	0.83	68	18.16[a]	52	39.23[a]	32
$t_{1/2}$ (h)	0.8	24	22.0[a]	45	76.3[a]	61
F_r	1	–	21.9	–	47.2	–

[a] Statistically significant increase when compared to the unprocessed drug ($p < 0.05$).

Fig. 9. Mean plasma concentration − time profiles following the oral administration of one single dose (10 mg/kg) of unprocessed IDV free base (●), pure IDV free base nanoparticles (▲) and film-coated NiMDS-28 (■) encapsulated within gastro-resistant capsules to mongrel dogs ($n = 4$).

intestinal mucosa by physical entrapment. Encapsulation of the nanoparticles improved the biopharmaceutical performance of the drug even more, with a 47-fold bioavailability increase and a prolongation of the apparent $t_{1/2}$ of 95 times. Furthermore, the use of all FDA-approved components and methodologies that are scalable under an industrial setting remarkably increases the possibility of bench-to-bedside translation of the first DDS developed for the oral controlled release of a PI. These findings not only support the use of this mucoadhesive release platform to reduce the frequency of administration (and increase patient compliance) of single state-of-the-art PIs such as the darunavir [49], but also of their combinations with the boosting agent ritonavir. Further studies will investigate the coating of the NiMDSs with an outer gastro-resistant film that withstands the gastric medium and that undergoes fast dissolution in the intestine, exposing a mucoadhesive polymer film. This approach would enable the administration of this novel DDS as a suspension in pediatric patients, a high-risk sub-population in HIV and other poverty-related diseases [50,51], without compromising the integrity of the microparticles, preventing the release of the encapsulated drug in the stomach and masking the bitter taste of these drugs that reduces patient compliance [52].

Acknowledgments

References

[1] HIV/AIDS Fact Sheet #360. World health organization. 2014. Available from: URL, http://www.who.int/mediacentre/factsheets/fs360/en/.

[2] Global. AIDS response progress reporting 2014, UNAIDS. 2014. Available from: URL, http://www.unaids.org/es/dataanalysis/knowyourepidemic/.

[3] Thompson MA, Aberg JA, Hoy JF, Telenti A, Benson C, Cahn P, et al. Antiretroviral treatment of adult HIV infection: 2012 recommendations of the International Antiviral Society-USA panel. J Am Med Assoc 2012;308:387–402.

[4] Andrews L, Friedland G. Progress in the HIV therapeutics and the challenges of adherence to antiretroviral therapy. Infect Dis Clin North Am 2000;14:1–26.

[5] Nicholson LK, Yamazaki T, Torchia DA, Grzesiek S, Bax A, Stahl SJ, et al. Flexibility and function in HIV-1 protease. Nat Struct Biol 1995;2:274–80.

[6] Kumar GN, Rodrigues AD, Buko AM, Denissen JF. Cytochrome P450-mediated metabolism of the HIV-1 protease inhibitor ritonavir (ABT-538) in human liver microsomes. J Pharmacol Exp Ther 1996;277:423–31.

[7] Ford J, Khoo SH, Back DJ. The intracellular pharmacology of antiretroviral protease inhibitors. J Antimicrob Chemother 2004;54:982–90.

[8] Hochman JH, Chiba M, Nishime J, Yamazaki M, Lin JH. Influence of P-glycoprotein on the transport and metabolism of indinavir in Caco-2 cells expressing cytochrome P-450 3A4. J Pharmacol Exp Ther 2000;292:310–8.

[9] Lee CG, Gottesman MM, Cardarelli CO, Ramachandra M, Jeang KT, Ambudkar SV, et al. HIV-1 protease inhibitors are substrates for the MDR1 multidrug transporter. Biochemistry 1998;37:3594–601.

[10] Kim RB, Fromm MF, Wandel C, Leake B, Wood AJ, Roden DM, et al. The drug transporter P-glycoprotein limits oral absorption and brain entry of HIV-1 protease inhibitors. J Clin Invest 1998;101:289–94.

[11] Profit L, Eagling VA, Back DJ. Modulation of P-glycoprotein function in human lymphocytes and Caco-2 cell monolayers by HIV-1 protease inhibitors. AIDS 1999;13:1623–7.

[12] Srinivas RV, Middlema D, Flynn P, Fridland A. Human immunodeficiency virus protease inhibitors serve as substrates for multidrug transporter proteins MDR1 and MRP1 but retain antiviral efficacy in cell lines expressing these transporters. Antimicrob Agents Chemother 1998;42:3157–62.

[13] *Antiretroviral drugs used in the treatment of HIV infection, US food and drug administration.* Available from: URL: http://www.fda.gov/forconsumers/byaudience/%20forpatientadvocates/ucm076940.htm.

[14] Boyd M. Indinavir: the forgotten HIV-protease inhibitor. Does it still have a role? Expert Opin Pharmacother 2007;8:957–64.

[15] Cahn P, On behalf of the GARDEL Study Group. Dual therapy with lopinavir/ritonavir (LPV/r) and lamivudine (3TC) is non-inferior to standard triple drug therapy in naïve HIV-1 infected subjects: 48-week results of the GARDEL study. In: 14th European AIDS conference of the European AIDS clinical society. Brussels: Belgium; 2013. Abstract LBPS7/6.

[16] Wu CY, Benet LZ. Predicting drug disposition via application of BCS: transport/absorption/elimination interplay and development of biopharmaceutics drug disposition classification system. Pharm Res 2005;22:11–23.

[17] Rittweger M, Arasteh K. Clinical pharmacokinetics of darunavir. Clin Pharmacokinet 2007;46:739–56.

[18] Sosnik A, Chiappetta DA, Carcaboso AM. Drug delivery systems in HIV pharmacotherapy: what has been done and the challenges standing ahead. J Control Release 2009;138:2–15.

[19] Imperiale JC, Sosnik A. Nanoparticle-in-microparticle delivery systems (NiMDS): production, routes of administration and clinical potential. J Biomater Tissue Eng 2013;3:22–38.

[20] Sosnik A, das Neves J, Sarmento B. Mucoadhesive polymers in the design of nano-drug delivery systems for administration by non-parenteral routes: A review. *Prog Polym Sci*, accepted.

[21] Toteva MM, Zanon R, Ostovic D. Kinetics and mechanism of the hydrolytic degradation of indinavir: intramolecular catalysis. J Pharm Sci 2008;97: 3810–9.

[22] Imperiale JC, Bevilacqua G, de Tarso Vieira e Rosa P, Sosnik A. Production of pure indinavir free base nanoparticles by a supercritical anti-solvent (SAS) method. Drug Dev Ind Pharm 2013. http://dx.doi.org/10.3109/03639045.2013.838581. Available from: URL, http://www.ncbi.nlm.nih.gov/pubmed/24050705.

[23] Phillips DJ, Pygall SR, Cooper B, Mann JC. Overcoming sink limitations in dissolution testing: a review of traditional methods and the potential utility of biphasic systems. J Pharm Pharmacol 2012;64:1549–59.

[24] Shah LK, Amiji MM. Intracellular delivery of saquinavir in biodegradable polymeric nanoparticles for HIV/AIDS. Pharm Res 2006;23:2638–45.

[25] Glisoni RJ, García-Fernández MJ, Pino M, Gutkind G, Moglioni A, Alvarez-Lorenzo C, et al. β-Cyclodextrin hydrogels for the ocular release of antibacterial thiosemicarbazones. Carbohydr Polym 2013;93:449–57.

[26] Lin JH, Chen IW, Vastag KJ, Ostovic D. pH-dependent oral absorption of L-735,524, a potent HIV protease inhibitor, in rats and dogs. Drug Metab Dispos 1995;23:730–5.

[27] Nithitanakool S, Pithayanukul P, Bourgeois S, Fessi H, Bavovada R. The development, physicochemical characterisation and in vitro drug release studies of pectinate gel beads containing Thai mango seed kernel extract. Molecules 2013;18:6504–20.

[28] The United States Pharmacopeia Convention, USP 33/701, Rockville M.D. 2008.

[29] McMillan CJ, Livingston A, Clark CR, Dowling PM, Taylor SM, Duke T, et al. Pharmacokinetics of intravenous tramadol in dogs. Can J Vet Res 2008;72: 325–31.

[30] Bramuglia GF, Cortada CM, Curras V, Hocht C, Buontempo F, Mato G, et al. Relationship between P-glycoprotein activity measured in peripheral blood mononuclear cells and indinavir bioavailability in healthy volunteers. J Pharm Sci 2009;98:327–36.

[31] Rabinow BE. Nanosuspensions in drug delivery. Nat Rev Drug Discov 2004;3: 785–96.

[32] Müller RH, Gohla S, Keck CM. State of the art of nanocrystals – special features, production, nanotoxicology aspects and intracellular delivery. Eur J Pharm Biopharm 2011;78:1–9.

[33] Seremeta KP, Chiappetta DA, Sosnik AD. Poly(ε-caprolactone), Eudragit® RS 100 and poly(ε-caprolactone)/Eudragit® RS 100 blend submicron particles for the sustained release of the antiretroviral efavirenz. Colloids Surf B Biointerfaces 2013;102:441–9.

[34] ICH Topic Q3C (R4). *Impurities: guideline for residual solvents, European Medicines Agency.* Available from: URL: http://www.tga.gov.au/pdf/euguide/ich28395enrev4.pdf.

[35] Glisoni RJ, Chiappetta DA, Finkielsztein LM, Moglioni AG, Sosnik A. Self-aggregation behaviour of novel thiosemicarbazone drug candidates with potential antiviral activity. New J Chem 2010;34:2047–58.

[36] Ferreira da Silva RM, Morais de Medeiros FP, Nascimento TG, Macedo RO, Neto PJR. J Therm Anal Calorim 2009;95:965–8.

[37] Andrade F, Goycoolea F, Chiappetta DA, das Neves J, Sosnik A, Sarmento B. Chitosan-grafted copolymers and chitosan-ligand conjugates as matrices for pulmonary drug delivery. Int J Carbohyd Chem 2011;2011. Art. 865704.

[38] Sosnik A. Alginate particles as platform for drug delivery by the oral route: State-of-the-Art. ISRN Pharm 2014;2014. Art. 926157.

[39] Pasparakis G, Bouropoulos N. Swelling studies and in vitro release of verapamil from calcium alginate and calcium alginate–chitosan beads. Int J Pharm 2006;323:34–42.

[40] Sankalia MG, Mashru RC, Sankalia JM, Sutariya VB. Reversed chitosan–alginate polyelectrolyte complex for stability improvement of alpha-amylase: optimization and physicochemical characterization. Eur J Pharm Biopharm 2007;65:215–32.

[41] Bajpai SK, Sharma S. Investigation of swelling/degradation behavior of alginate beads crosslinked with Ca²⁺ and Ba²⁺ ions. React Funct Polym 2004;59: 129–40.

[42] Dillen K, Vandervoort J, Van den Mooter G, Ludwig A. Evaluation of ciprofloxacin-loaded Eudragit RS100 or RL100/PLGA nanoparticles. Int J Pharm 2006;314:72–82.

[43] Davidovich-Pinhas M, Bianco-Peled H. Mucoadhesion: a review of characterization techniques. Expert Opin Drug Deliv 2010;7:259–71.

[44] Hung S-F, Hsieh C-M, Chen Y-C, Wang Y-C, Ho H-O, Sheu M-T. Characterizations of plasticized polymeric film coatings for preparing multiple-unit floating drug delivery systems (muFDDSs) with controlled-release characteristics. PLOS One 2014;9:e100321.

[45] das Neves J, Bahia MF, Amiji MM, Sarmento B. Mucoadhesive nanomedicines: characterization and modulation of mucoadhesion at the nanoscale. Expert Opin Drug Deliv 2011;7:1085–104.

[46] Bastakoti BP, Guragain S, Yokoyama Y, Yusa S, Nakashima K. Incorporation and release behavior of amitriptylene in core-shell-corona type triblock copolymer micelles. Colloids Surf B: Biointerfaces 2011;88:734–40.

[47] Puga AM, Rico-Rey A, Magariños B, Alvarez-Lorenzo C, Concheiro A. Hot melt poly-ε-caprolactone/poloxamine implantable matrices for sustained delivery of ciprofloxacin. Acta Biomater 2012;8:1507–18.

[48] Burger D, Boyd M, Duncombe C, Felderhof M, Mahanontharit A, Ruxrungtham K, et al. Pharmacokinetics and pharmacodynamics of indinavir with or without low-dose ritonavir in HIV-infected Thai patients. J Antimicrob Chemother 2003;51:1231–8.

[49] Glisoni RJ, Sosnik A. Novel poly(ethylene oxide)-co-poly(propylene oxide) copolymer-glucose conjugate by the microwave-assisted ring opening of a sugar lactone. Macromol Biosci 2014. http://dx.doi.org/10.1002/mabi.201400235. in press.

[50] Sosnik A, Seremeta KP, Imperiale JC, Chiappetta DA. Novel formulation and drug delivery strategies for the treatment of pediatric poverty related diseases (PRDs). Expert Opin Drug Deliv 2012;9:303–23.

[51] Sosnik A, Carcaboso A. Nanomedicines in the future of pediatric therapy. Adv Drug Deliv Rev 2014;73:140–61.

[52] Chiappetta DA, Carcaboso AM, Bregni C, Rubio MC, Bramuglia G, Sosnik A. Indinavir-loaded ph-sensitive microparticles for taste masking: towards extemporaneous paediatric HIV/AIDS liquid formulations with improved patient compliance. AAPS PharmSciTech 2009;10:1–6.